ELSEVIER

Finite Elements in Analysis and Design 37 (2001) 199–219

FINITE ELEMENTS IN ANALYSIS AND DESIGN

www.elsevier.com/locate/finel

Dynamic response of spinning tapered Timoshenko beams using modal reduction

A. Bazoune[a,*], Y.A. Khulief[a], N.G. Stephen[b], M.A. Mohiuddin[c]

[a]*Department of Mechanical Engineering, King Fahd University of Petroleum and Minerals, KFUPM Box #579, Dhahran 31261, Saudi Arabia*

[b]*Department of Mechanical Engineering, University of Southampton, Southampton SO17 1BJ, UK*

[c]*Center for Petroleum & Minerals, Research Institute, King Fahd University of Petroleum and Minerals, KFUPM Box #755, Dhahran 31261, Saudi Arabia*

Abstract

A method for dynamic response analysis of spinning tapered Timoshenko beams utilizing the finite element method is developed. The equations of motion are derived to include the effects of Coriolis forces, shear deformation, rotary inertia, hub radius, taper ratios and angular setting of the beam. Modal transformations from the space of nodal coordinates to the space of modal coordinates are invoked to alleviate the problem of large dimensionality resulting from the finite element discretization. Both planar and complex modal transformations are presented and applied. The reduced order modal form of equations of motion is computer generated, integrated forward in time, and the system dynamic response is evaluated. Numerical results and comparisons with the full order model (FOM) are presented to demonstrate the accuracy of the reduced order model (ROM).

Keywords: Dynamic response analysis; Timoshenko beams; Modal reduction

1. Introduction

The dynamic analysis of spinning structures has attracted several investigators to intensive study over the past four decades in order to improve their efficiency and dynamic characteristics. Rotating beams-like components fall into this category of structures and are widely used in various fields, such as rotating machinery, space satellites and helicopter blades.

A large number of studies were dedicated to study the dynamic behavior of rotating uniform or tapered Euler–Bernoulli beams [1–7]. Few investigators have tackled the problem of rotating

* Corresponding author.

0168-874X/01/$ - see front matter
PII: S0168-874X(00)00030-5

beams including rotary inertia and shear deformation effects. Such factors are crucial to the dynamic behavior of rotating short beams which comprise a basic component in many engineering applications. Boutaghou and Erdman [8] derived the equations of motion of rotating elastic structures using Hamilton's principle with the von Kármán geometric constraint to capture the centrifugal stiffening effect arising in fast rotating structures. They applied this approach in conjunction with the finite element method (FEM). Kane et al. [9] studied the behavior of a cantilever beam built into a rigid body that is performing specified motion of rotation and translation. Chen and Chen [10] used the finite element model presented by Thomas and Abbas [11] and incorporated the effect of rotation introduced by Carnegie [12] to study the transient response of a rotating blade of generally orthotropic materials. Bakr and Shabana [13] investigated the behavior of Timoshenko beams in multibody systems consisting of interconnected rigid and deformable bodies each of which may undergo finite rotations. It was shown therein that the inclusion of rotary inertia and shear deformation has a significant effect on the dynamic response of flexible multibody systems. Later, Wei-Hsin and Shabana [14] developed a dynamic formulation for initially curved Timoshenko beams that undergo finite rotations. To show an application of their formulation, the authors used a multibody slider crank mechanism with flexible links.

The FEM is the most powerful numerical technique that has great potential and flexibility in modeling complex and large structures. However, utilizing nodal coordinates in the discretization process leads to a large number of degrees of freedom of the model, and consequently, results in a large number of dynamic equations for which a solution becomes impracticable. Moreover, the use of nodal coordinates results in a dynamic model of widely spread eigen-spectrum that includes many insignificant modes and consequently, a numerically stiff system is often created which causes the numerical integration scheme to search inefficiently for a solution or may even fail to find one.

Using modal coordinates alleviates the problem of large dimensionality incurred by using nodal coordinates, and avoids the inclusion of higher insignificant modes when they do not share an appreciable amount of the system's kinetic energy [15]. In general, a subset of eigenvectors which spans the frequency spectrum of the forcing function are retained as significant modes.

The distinction between significant and insignificant modal coordinates leads to a convenient formulation of the reduced order model by means of a reduction technique referred to as mass condensation [16], in which it is assumed that the mass of the structure can be lumped at only specific degrees of freedom. The disadvantages of this technique is that the banded nature of the original system may be destroyed and may lead to a much more expensive eigensolution. In addition, the inertia matrix is sometimes singular because of the presence of massless degree of freedom which may cause the eigensolver to fail. Several investigations related to mass condensation have been reported in the literature [16–22].

Hurty [23], Craig and Bampton [24] and Benfield and Hruda [25] used the component modes to analyze complex structural systems. Based on substructuring, this approach couples various components of a structure to predict the dynamic behavior of the entire structure. Ojalvo and Newman [26] presented a matrix-reduction method to predict the frequencies of vibration of large structures by solving an eigenvalue problem of smaller size than the actual one.

Laurenson [27] addressed the issue of reduction techniques and indicated the revisions that should be considered when the FEM is used in dynamic analysis of flexible structures that include the effect of spinning. In [28], Likins developed a general study in which he provided the governing equations for flexible appendages and outlined the steps that should be followed in conjunction

with the FEM formulation in order to reduce the size of the original structure by means of a modal transformation. Shabana and Wehage [29] extended the coordinate reduction technique to spatial substructures with large angular rotations. Kane and Torby [30] applied the extended modal reduction method to solve the eigenvalue problem of a simple rotor problem using state space formulation to allow for non-symmetric matrices such that damping, and gyroscopic effects may be treated. However, the authors in [30] did not perform any dynamic analysis. Later, Khulief and Mohiuddin [31] used the complex modal reduction technique in rotor dynamic response analysis in which they included the gyroscopic moments and anisotropic bearing effects.

In the current literature, the problem of dynamic analysis of spinning tapered Timoshenko beams utilizing the actual complex modal reduction has not yet been reported. Tapered Timoshenko beam-like structures are widely encountered in many engineering applications and represent basic components in rotors and space structures. It is however, the purpose of this investigation to develop a nonlinear dynamic finite element formulation of rotating tapered Timoshenko beams. The formulation is based on the principle of virtual work. The nonlinear terms that represent the inertia coupling between the reference motion and small elastic deformations are expressed in terms of a set of time invariant quantities (scalars and matrices) that depend on the assumed displacement field, rotary inertia, shear deformation, setting angle, hub radius and taper ratios. The use of this nonlinear formulation is demonstrated first by casting the system equations in state space form in order to accommodate the Coriolis effects. Both planar and complex modal transformations are presented and applied to obtain a reduced order model. The reduced order modal form of equations of motion is computer generated, integrated forward in time, and the system dynamic response is evaluated for different types of external loading conditions. Numerical examples are presented to demonstrate the validity and efficiency of the developed computational scheme.

2. The beam element model

Fig. 1 shows a typical rotating tapered cantilever beam model in the deformed state. In this figure, the (XYZ) axes represent a global orthogonal coordinate system with origin at the center of mass of the hub such that the Z-axis corresponds to the spin axis which rotates with a constant angular speed $\dot{\phi} = \Omega$. The $(X'Y'Z')$ system is defined as a system of local coordinates parallel to the global (XYZ) coordinate system and rigidly attached to the root of the beam with its origin shifted by $\mathscr{R}_0$ from the global (XYZ) coordinate system. The coordinate system (xyz) represents a body coordinate system that is rigidly attached to the root of the beam and is obtained by rotating the $(X'Y'Z')$ coordinate system about X'-axis by an angle ψ called setting angle. The X, X' and x axes being collinear and coincident with the undeformed beam centerline while the y- and z-axis lie along the principal axes of the cross-sectional area of the beam. The beam undergoes flexural vibration in a plane fixed in a local system and rotating with the beam. For $\psi = 90°$, the vibration is in the plane of rotation and for $\psi = 0°$, the vibration is out of the plane of rotation.

The beam configuration can be defined by a properly generated mesh of finite beam elements. These beam elements are linearly tapered in two planes while allowing for unequal breadth and width taper ratios as well as unequal element lengths. Each element has a length l such that the length of the beam is the summation of its individual element lengths. Each beam element consists

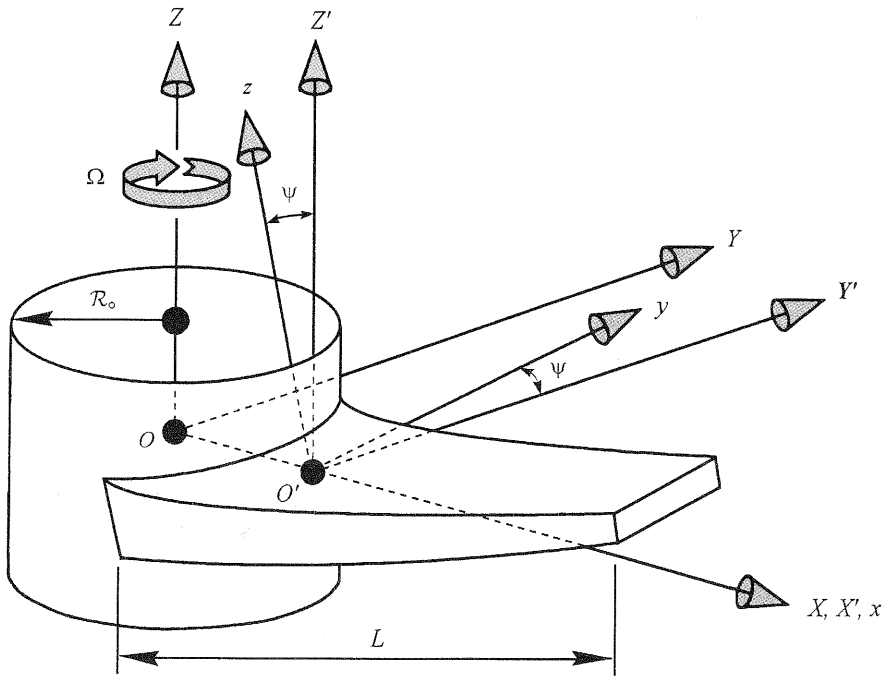

Fig. 1. The rotating tapered beam configuration in the deformed state.

of two nodes and each node is represented by four degrees of freedom, a transverse and axial displacements and torsional and bending rotations; so the beam element has eight nodal coordinates or simply eight elastic degrees of freedom. Effects of Coriolis forces, shear deformation, rotary inertia, hub radius, angular setting, taper ratios in (xy) and (xz) planes and spinning of the hub are considered in this investigation.

3. Kinematic relations

Referring to Fig. 2, the global position vector of an arbitrary point P on the beam can be defined with respect to the global (XYZ) coordinates system as

$$\{R_P\} = \{\mathscr{R}_o\} + [\mathscr{A}]\{r_P\}, \tag{1}$$

where $\{\mathscr{R}_o\} = [X_o, 0, 0]^T$ is the location of the origin of the body coordinate system relative to the global coordinate system, $\{R_P\}$ is the global position of the reference point, and $\{r_P\}$ is the vector from the origin of the body coordinate system to point P in the deformed state. $[\mathscr{A}]$ is the coordinate transformation matrix that defines the orientation of the beam local coordinates with respect to the global coordinates. The vector $\{r_P\}$ can be expressed as

$$\{r_P\} = \{r_{P_o}\} + \{d\} = \{r_{P_o}\} + [\mathscr{N}]\{e\}, \tag{2}$$

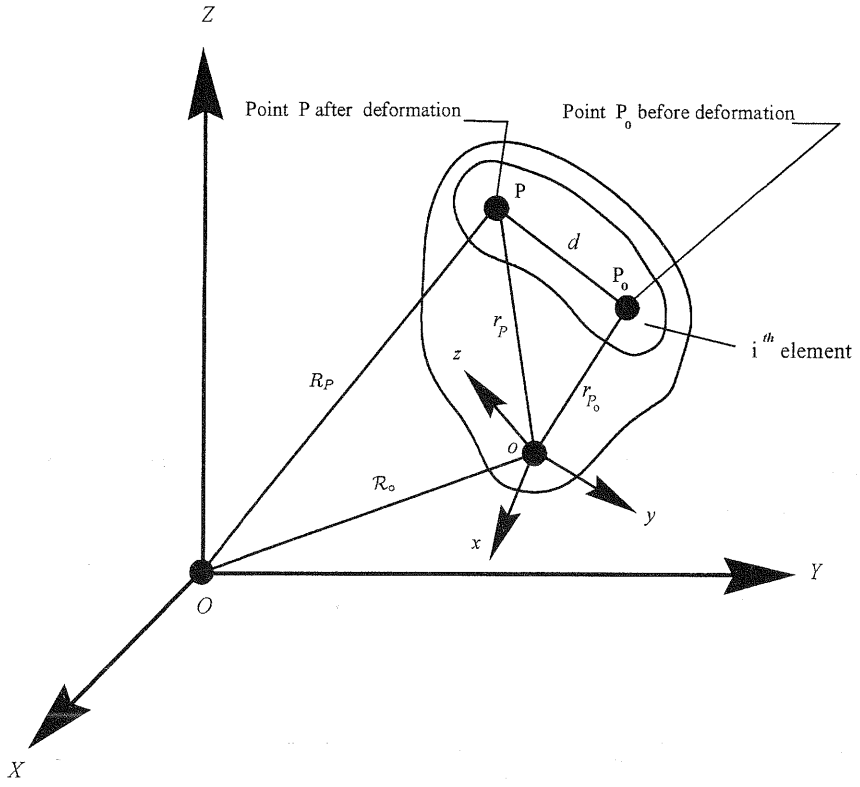

Fig. 2. Generalized coordinates of the ith beam element.

where $\{r_{P_o}\} = [x_o, 0, 0]^T$ is the position vector of the point P with respect to the reference point in the undeformed state. The vector $\{d\}$ is the elastic deformation vector which gives the difference between the deformed and undeformed state vectors $\{r_P\}$ and $\{r_{P_o}\}$, respectively. The vector $\{e\}$ is the vector of elastic coordinates. The matrix $[\mathcal{N}]$ is the composite matrix of shape functions $[\mathcal{N}_a]$, $[\mathcal{N}_w]$, $[\mathcal{N}_{\theta_x}]$ and $[\mathcal{N}_{\theta_y}]$ used to model the axial, bending translation, torsion and bending rotational deformations, respectively, of the beam element. By substituting Eq. (2) into (1), one gets

$$\{R_P\} = \{\mathcal{R}_o\} + [\mathcal{A}](\{r_{P_o}\} + [\mathcal{N}]\{e\}). \tag{3}$$

Differentiating this equation with respect to time, one obtains

$$\{\dot{R}_P\} = \{\dot{\mathcal{R}}_o\} + [\dot{\mathcal{A}}](\{r_{P_o}\} + [\mathcal{N}]\{e\}) + [\mathcal{A}][\mathcal{N}]\{\dot{e}\}, \tag{4}$$

which can be written as

$$\{\dot{R}_p\} = [[\tilde{\mathcal{A}}_I]\{\mathcal{R}_o\} + [\mathcal{A}_\varphi](\{r_{P_o}\} + [\mathcal{N}]\{e\}) \quad [\mathcal{A}][\mathcal{N}]]\begin{Bmatrix} \dot{\varphi} \\ \{\dot{e}\} \end{Bmatrix} = [\boldsymbol{L}]\{\dot{q}\}, \tag{5}$$

where $[\mathscr{A}_\varphi]$ is the partial derivative of the transformation matrix $[\mathscr{A}]$ with respect to the orientation coordinate φ, while $[\tilde{\mathscr{A}}_I]$ is a skew-symmetric matrix given by

$$[\tilde{\mathscr{A}}_I] = \begin{bmatrix} 0 & -1 \\ 1 & 0 \end{bmatrix} \tag{6}$$

and $[\boldsymbol{L}]$ is defined as

$$[\boldsymbol{L}] = [[\tilde{\mathscr{A}}_I]\{\mathscr{R}_o\} + [\mathscr{A}_\varphi](\{r_{P_o}\} + [\mathscr{N}]\{e\}) \quad [\mathscr{A}][\mathscr{N}]], \tag{7}$$

and

$$\{\dot{q}\} = \begin{Bmatrix} \dot{\varphi} \\ \{\dot{e}\} \end{Bmatrix}. \tag{8}$$

The time derivative of the absolute velocity represents the absolute acceleration which is defined as

$$\{\ddot{R}_p\} = [\boldsymbol{L}]\{\ddot{q}\} + [\dot{\boldsymbol{L}}]\{\dot{q}\}. \tag{9}$$

4. Inertia forces

The virtual displacement of an arbitrary point on the beam can be written as

$$\delta\{R_P\} = [\boldsymbol{L}]\delta\{q\} \tag{10}$$

and the virtual work of the inertia forces can be written as

$$\delta\{W_i\} = \int_V \rho\{\ddot{R}_P\}^T \delta\{R_P\}\,dV = \int_V \rho\{\{\ddot{q}\}^T[\boldsymbol{L}]^T + \{\dot{q}\}^T[\dot{\boldsymbol{L}}]^T\}[\boldsymbol{L}]\delta\{q\}\,dV, \tag{11}$$

where ρ is the mass density and V is the volume of the beam. Eq. (11) can be written as

$$\delta\{W_i\} = [[M]\{\ddot{q}\} - \{Q_v\}]^T\delta\{q\}, \tag{12}$$

where $[M]$ is the symmetric mass matrix of the beam and is given by

$$[M] = \begin{bmatrix} [M_{rr}] & [M_{rf}] \\ [M_{fr}] & [M_{ff}] \end{bmatrix} = \int_V \rho[\boldsymbol{L}]^T[\boldsymbol{L}]\,dV \tag{13}$$

in which $[M_{fr}] = [M_{rf}]^T$. The submatrix $[M_{rr}]$ is the mass matrix associated with reference coordinates, usually referred to as mass matrix due to rigid body rotation, while the submatrix $[M_{rf}]$ represents the inertia coupling between the reference motion and the elastic deformations of the beam. The submatrix $[M_{ff}]$ associated with the elastic coordinates is of the kind usually occurring in linear structural dynamics problems and comprises all the matrices associated with the elastic generalized coordinates. This submatrix is invariant and can be evaluated once in advance in dynamic analysis. Unlike $[M_{ff}]$, the submatrices $[M_{rr}]$ and $[M_{rf}]$ are implicitly time dependent since they are function of the generalized coordinates thus resulting in an inertia variant

model. The elements of the mass matrix $[M]$ are given by

$$[M_{rr}] = [\boldsymbol{I}_{\mathscr{R}_o\mathscr{R}_o}] + [\boldsymbol{I}_{\mathscr{R}_o r_{P_o}}] + [\boldsymbol{I}_{r_{P_o} r_{P_o}}] + [m_{\mathscr{R}_o e}]^{\mathrm{T}}\{e\} + [m_{r_{P_o} e}]^{\mathrm{T}}\{e\} + \{e\}^{\mathrm{T}}[m_{ee}]\{e\}, \tag{14}$$

$$[M_{rf}] = [m_{\mathscr{R}_o}]^{\mathrm{T}} + [m_{r_{P_o}}]^{\mathrm{T}} + \{e\}^{\mathrm{T}}[\tilde{C}]^{\mathrm{T}}, \tag{15}$$

$$[M_{ff}] = \int_V \rho[\mathscr{N}]^{\mathrm{T}}[\mathscr{N}]\,\mathrm{d}V, \tag{16}$$

in which

$$[\boldsymbol{I}_{\mathscr{R}_o\mathscr{R}_o}] = \int_V \rho\{\mathscr{R}_o\}^{\mathrm{T}}\{\mathscr{R}_o\}\,\mathrm{d}V, \tag{17}$$

$$[\boldsymbol{I}_{\mathscr{R}_o r_{P_o}}] = \int_V \rho\{\mathscr{R}_o\}^{\mathrm{T}}[\tilde{\mathscr{A}}_I]^{\mathrm{T}}[\mathscr{A}_\varphi]\{r_{P_o}\}\,\mathrm{d}V, \tag{18}$$

$$[\boldsymbol{I}_{r_{P_o} r_{P_o}}] = \int_V \rho\{r_{P_o}\}^{\mathrm{T}}\{r_{P_o}\}\,\mathrm{d}V, \tag{19}$$

$$[m_{\mathscr{R}_o e}] = \int_V \rho[\mathscr{N}]^{\mathrm{T}}[\mathscr{A}_\varphi]^{\mathrm{T}}[\tilde{\mathscr{A}}_I]\{\mathscr{R}_o\}\,\mathrm{d}V, \tag{20}$$

$$[m_{r_{P_o} e}] = \int_V \rho[\mathscr{N}]^{\mathrm{T}}\{r_{P_o}\}\,\mathrm{d}V, \tag{21}$$

$$[m_{ee}] = \int_V \rho[\mathscr{N}_w]^{\mathrm{T}}[\mathscr{N}_w]\,\mathrm{d}V, \tag{22}$$

$$[m_{\mathscr{R}_o}] = \int_V \rho[\mathscr{N}]^{\mathrm{T}}[\mathscr{A}]^{\mathrm{T}}[\tilde{\mathscr{A}}_I]\{\mathscr{R}_o\}\,\mathrm{d}V, \tag{23}$$

$$[m_{r_{P_o}}] = \int_V \rho[\mathscr{N}]^{\mathrm{T}}[\mathscr{A}]^{\mathrm{T}}[\mathscr{A}_\varphi]\{r_{P_o}\}\,\mathrm{d}V, \tag{24}$$

$$[\tilde{C}] = \int_V \rho[\mathscr{N}]^{\mathrm{T}}[\tilde{\mathscr{A}}_I][\mathscr{N}]\,\mathrm{d}V, \tag{25}$$

$$[M_{ff}] = \int_V \rho[\mathscr{N}]^{\mathrm{T}}[\mathscr{N}]\,\mathrm{d}V. \tag{26}$$

5. Coriolis and centrifugal forces

Using Eqs. (11) and (12), $\{Q_v\}$ is the quadratic velocity inertia force vector that includes the centrifugal and Coriolis forces and is defined as

$$\{Q_v\} = \begin{Bmatrix}\{Q_v\}_\varphi \\ \{Q_v\}_f\end{Bmatrix} = -\int_V \rho[\boldsymbol{L}]^{\mathrm{T}}[\dot{\boldsymbol{L}}]\{\dot{q}\}\,\mathrm{d}V \tag{27}$$

where $\{Q_v\}_\varphi$ represents the Coriolis forces associated with the beam reference rotation while $\{Q_v\}_f$ represents the centrifugal and Coriolis forces associated with the elastic degrees of freedom of the beam. The respective expressions of $\{Q_v\}_\varphi$ and $\{Q_v\}_f$ are given by

$$\{Q_v\}_\varphi = -2\Omega([m_{\mathscr{R}_o e}]^{\mathrm{T}} + [m_{r_{P_o} e}]^{\mathrm{T}} + \{e\}^{\mathrm{T}}[m_{ee}])\{\dot{e}\} - \Omega^2\{e\}^{\mathrm{T}}[\tilde{C}]\{e\}, \tag{28}$$

$$\{Q_v\}_f = ([m_{\mathscr{R}_o e}] + [m_{r_{P_o} e}] + [m_{ee}]\{e\})\Omega^2 - 2\Omega[\tilde{C}]\{\dot{e}\}. \tag{29}$$

6. Equations of motion of the model

The matrix form of the equations of motion of the spinning undamped and tapered Timoshenko beam can be written in terms of the generalized coordinates as

$$\begin{bmatrix}[M_{rr}] & [M_{rf}]\\ [M_{fr}] & [M_{ff}]\end{bmatrix}\begin{Bmatrix}\ddot{\varphi}\\ \ddot{e}\end{Bmatrix} + \begin{bmatrix}0 & 0\\ 0 & [K]\end{bmatrix}\begin{Bmatrix}\varphi\\ e\end{Bmatrix} = \begin{Bmatrix}\{Q_{ext}\}_\varphi + \{Q_v\}_\varphi\\ \{Q_{ext}\}_f + \{Q_v\}_f\end{Bmatrix}, \tag{30}$$

where $\{Q_{\mathrm{ext}}\}$ and $\{Q_{\mathrm{v}}\}$ are, respectively, the vector of the external applied forces and the vector of Coriolis and centrifugal forces. The matrix $[K]$ is the stiffness matrix defined as

$$[K] = [K_{ff}] + \Omega^2[K_c] \tag{31}$$

in which $[K_{ff}]$ denotes the elastic stiffness matrix while $[K_c]$ denotes the stiffness matrix due to the presence of rotation.

By considering the case of a beam rotating with a constant spin and by neglecting the coupling between the reference motion and elastic deformation such that $\ddot{\varphi} = 0$, $\{Q_{\mathrm{ext}}\}_\varphi = 0$ and $[M_{rf}] =$ null matrix, the equations of motion of the beam can be written as

$$[M_{ff}]\{\ddot{e}\} + ([K_{ff}] + \Omega^2[K_c])\{e\} = \{Q_{\mathrm{ext}}\}_f + \{Q_{\mathrm{v}}\}_f \tag{32}$$

or

$$[M_{ff}]\{\ddot{e}\} + 2\Omega[\tilde{C}]\{\dot{e}\} + ([K_{ff}] + \Omega^2([K_c] - [m_{ee}]))\{e\} = \{Q_{\mathrm{ext}}\}_f + ([m_{\mathscr{R}_o e}] + [m_{r_{P_o} e}])\Omega^2, \tag{33}$$

which is the equation of motion describing the in-plane ($\psi = 90°$) forced vibration of the spinning beam. For the out-of-plane vibration, however, the softening term $\Omega^2[m_{ee}]$ is dropped, and for a setting angle ψ, the equation of motion is written as [32,33]

$$[M_{ff}]\{\ddot{e}\} + 2\Omega[\tilde{C}]\{\dot{e}\} + ([K_{ff}] + \Omega^2([K_c] - [m_{ee}]\sin^2\psi))\{e\} = \{Q_{\mathrm{ext}}\}_f + ([m_{\mathscr{R}_o e}] + [m_{r_{P_o} e}])\Omega^2, \tag{34}$$

which can be written in compact form as

$$[M_{ff}]\{\ddot{e}\} + 2\Omega[\tilde{C}]\{\dot{e}\} + [\bar{K}]\{e\} = \{\bar{Q}\}, \tag{35}$$

where the matrices $[M_{ff}]$, $[\tilde{C}]$ and $[\bar{K}]$ are constant coefficient matrices in which the mass matrix and the modified stiffness matrix are symmetric and the Coriolis matrix is skew symmetric. The modified stiffness matrix is given by

$$[\bar{K}] = [K_{ff}] + \Omega^2([K_c] - [m_{ee}]\sin^2\psi) \tag{36}$$

while the vector

$$\{\bar{Q}\} = \{Q_{\text{ext}}\}_f + ([m_{\mathscr{R}_o e}] + [m_{r_{P_o} e}])\Omega^2 \tag{37}$$

is the vector of time-dependent external forces and absorbs the quadratic velocity terms $[m_{\mathscr{R}_o e}]\Omega^2$ and $[m_{r_{P_o} e}]\Omega^2$. The expression of $[m_{r_{P_o} e}]$ is now given by

$$[m_{r_P e}] = \int_V \rho[N]^{\mathrm{T}}[\mathscr{A}_o]\{r_{P_o}\}\,\mathrm{d}V, \tag{38}$$

where $[\mathscr{A}_o]$ is a constant transformation which accounts for the angular setting of the beam.

The assembled set of the system equations can be written as

$$[\boldsymbol{M}_{ff}]\{\ddot{e}\} + 2\Omega[\tilde{\boldsymbol{C}}]\{\dot{e}\} + [\bar{\boldsymbol{K}}]\{e\} = \{\bar{\boldsymbol{Q}}\}, \tag{39}$$

where $[\boldsymbol{M}_{ff}]$, $[\tilde{\boldsymbol{C}}]$ and $[\bar{\boldsymbol{K}}]$ are the global mass, Coriolis and stiffness matrix, respectively, while $\{\bar{\boldsymbol{Q}}\}$ is the global force vector of the entire beam obtained by the standard finite element assembly procedure.

7. Modal reduction schemes

In order to formulate the dynamic equations for the eigenvalue problem, the forcing vector $\{\bar{\boldsymbol{Q}}\}$ is dropped from Eq. (39), thus resulting in the following homogeneous part of the dynamic equation:

$$[\boldsymbol{M}_{ff}]\{\ddot{e}\} + 2\Omega[\tilde{\boldsymbol{C}}]\{\dot{e}\} + [\bar{\boldsymbol{K}}]\{e\} = \{\boldsymbol{0}\}. \tag{40}$$

The truncation operation aims at eliminating the insignificant modes which are, in general, higher modes that do not contain an appreciable amount of the system's kinetic energy. In general, a subset of eigenvectors which spans the frequency spectrum of the forcing function are retained as significant modes. Moreover, the retained modes must include the first few lower ones in terms of which the characteristics of the system must be preserved.

Two modal reduction schemes are established. The first scheme utilizes planar modes obtained by solving the self-adjoint eigenvalue, while the second scheme invokes the complex modes of the non-self-adjoint eigenvalue. In each case, a reduced order modal form of the equations of motion is obtained.

7.1. Planar modal transformation

In order to obtain the real eigenvalues and the associated planar modes, one must ignore the Coriolis matrix $[\tilde{C}]$ in Eq. (40). To this end, the associated homogenous adjoint equation can be written as

$$[M_{ff}]\{\ddot{e}\} + [\bar{K}]\{e\} = \{0\}. \tag{41}$$

Upon solving the self-adjoint eigenvalue problem associated with Eq. (41), one obtains a set of real eigenvalues and eigenvectors. Let $[\phi]$ denote the modal matrix that comprises a selected subset of the resulting real eigenvectors (planar modes). Now, a transformation from nodal coordinate space to modal coordinate space can be defined as

$$\{e\} = [\phi]\{\eta\}, \tag{42}$$

where $\{\eta\}$ is the vector of modal coordinates. If a reduced truncated set of significant modes are retained, the corresponding truncated form of Eq. (39) can be written as

$$[\phi]^{\mathrm{T}}[M_{ff}][\phi]\{\ddot{\eta}\} + 2\Omega[\phi]^{\mathrm{T}}[\tilde{C}][\phi]\{\dot{\eta}\} + [\phi]^{\mathrm{T}}[\bar{K}][\phi]\{\eta\} = [\phi]^{\mathrm{T}}\{\bar{Q}\} \tag{43}$$

or simply

$$[M_{ffr}]\{\ddot{\eta}\} + 2\Omega[\tilde{C}_r]\{\dot{\eta}\} + [\bar{K}_r]\{\eta\} = \{\bar{Q}_r\}, \tag{44}$$

where $[M_{ffr}]$, $[\tilde{C}_r]$, $[\bar{K}_r]$ and $\{\bar{Q}_r\}$ are the reduced modal mass, Coriolis, and stiffness matrices, and reduced modal force vector, respectively. Eq. (44) represents the planar reduced order model (PROM) using planar modal reduction.

7.2. Complex modal transformation

In this case, the equation of motion (39) is first represented in the state-space form as

$$[A]\{\dot{y}\} + [B]\{y\} = \{F\} \tag{45}$$

in which

$$[A] = \begin{bmatrix} [0] & -[M_{ff}] \\ [M_{ff}] & 2\Omega[\tilde{C}] \end{bmatrix}, \tag{46}$$

$$[B] = \begin{bmatrix} [M_{ff}] & [0] \\ [0] & [\bar{K}] \end{bmatrix} \tag{47}$$

and

$$\{y\} = \begin{Bmatrix} \{\dot{e}\} \\ \{e\} \end{Bmatrix}, \tag{48}$$

where the matrix $[B]$ is symmetric while the matrix $[A]$ is skew-symmetric. Notice that if the dimensions of $[M_{ff}]$, $[\bar{K}]$ and $[\tilde{C}]$ are $(4n \times 4n)$ where n is the number of nodes, the dimensions of

$[A]$ and $[B]$ are $(8n \times 8n)$. The force vector on the right-hand side of Eq. (45) is given by

$$\{F\} = \begin{Bmatrix} \{0\} \\ \{\bar{Q}\} \end{Bmatrix}. \tag{49}$$

The two homogeneous adjoint equations can be written as

$$[A]\{\dot{y}\} + [B]\{y\} = \{0\} \tag{50}$$

and

$$[A]^{\mathrm{T}}\{\dot{y}\}' + [B]^{\mathrm{T}}\{y\}' = \{0\}. \tag{51}$$

Assuming a solution of the form

$$\{y\} = \{\bar{y}\}\exp(i\bar{\omega}t), \tag{52}$$

where $\{\bar{y}\}$ is the vector of displacement amplitudes and $\bar{\omega}$ is the frequency of harmonic vibrations and $i = \sqrt{-1}$. Substituting Eq. (52) into Eqs. (50) and (51), one can write

$$(\lambda_i[A] + [B])\{\Re_i\} = \{0\} \tag{53}$$

and

$$(\lambda_i[A]^{\mathrm{T}} + [B]^{\mathrm{T}})\{\mathscr{L}_i\} = \{0\} \tag{54}$$

where $\lambda_i = \pm i\bar{\omega}_i$ denotes the ith eigenvalue associated with right- and left-hand eigenvectors $\{\Re_i\}$ and $\{\mathscr{L}_i\}$, respectively. For symmetric $[A]$ and $[B]$, the eigenvectors $\{\Re_i\}$ and $\{\mathscr{L}_i\}$ are equal, otherwise $\{\Re_i\}$ and $\{\mathscr{L}_i\}$ are distinct.

Let $[\Re]$ and $[\mathscr{L}]$ denote the complex modal matrices for the differential operators of Eqs. (50) and (51), respectively. Introducing the transformation [35]

$$\{y\} = [\Re]\{u\}, \tag{55}$$

where $\{u\}$ is the vector of modal coordinates. If only a subset of significant modes are to be retained, the truncated modal form of the equations of motion can be written as

$$[\mathscr{L}]^{\mathrm{T}}[A][\Re]\{\dot{u}\} + [\mathscr{L}]^{\mathrm{T}}[B][\Re]\{u\} = [\mathscr{L}]^{\mathrm{T}}\{F\}, \tag{56}$$

where $[\Re]$ and $[\mathscr{L}]$ contain only those complex eigenvectors that represent a subset of selected modes. Eq. (56) can be written as

$$[A_{\mathrm{r}}]\{\dot{u}\} + [B_{\mathrm{r}}]\{u\} = \{F_{\mathrm{r}}\}, \tag{57}$$

where $[A_{\mathrm{r}}]$, $[B_{\mathrm{r}}]$ and $\{F_{\mathrm{r}}\}$ represent reduced $[A]$ and $[B]$ matrices, and reduced modal force vector, respectively. Eq. (57) represents the complex reduced order model (CROM) using complex modal reduction.

Eqs. (44) and (57) represent truncated models using planar and complex modal transformations, respectively. In general, a subset of eigenvectors which spans the frequency spectrum of the forcing function are retained as significant modes. Deciding on which modes to retain is not clear in most situations of dynamic response analysis. As a minimum requirement the retained modes must span the low-frequency subsystem in addition to any higher modes spanned by the frequency spectrum of the forcing function.

Table 1
The first six frequency parameters of rotating uniform Timoshenko beam $(r_g/L) = 0.02$, $\mathscr{R}_o = 0$, and $\psi = 0°$

$\bar{\Omega}$	λ_i	Planar modes	Complex modes	Ref. [34]	Exact value [34]
0	λ_1	3.5026405	—	3.5026	3.5026
	λ_2	21.4733106	—	21.4698	21.4698
	λ_3	47.8319424[a]	—	—	—
	λ_4	58.2278625	—	58.1498	58.1498
	λ_5	78.5959016[b]	—	—	—
	λ_6	109.5477733	—	109.0275	109.0275
3	λ_1	4.7822099	$\pm$ 4.7820661i	4.7947	4.7803
	λ_2	22.7669495	$\pm$ 22.7662115i	22.7551	22.7599
	λ_3	47.8319424[a]	$\pm$ 47.8326614i[a]	—	—
	λ_4	59.5481442	$\pm$ 59.5485000i	59.4491	59.4681
	λ_5	78.5959016[b]	$\pm$ 78.5959016i[b]	—	—
	λ_6	110.955603	$\pm$ 110.9553748i	110.3938	110.4310
6	λ_1	7.3361371	$\pm$ 7.3359489i	7.4261	7.3319
	λ_2	26.2642362	$\pm$ 26.2603567i	26.2243	26.2488
	λ_3	47.8319424[a]	$\pm$ 47.8362932i[a]	—	—
	λ_4	63.3232643	$\pm$ 63.3238549i	63.0795	63.2386
	λ_5	78.5959016[b]	$\pm$ 78.5959016i[b]	—	—
	λ_6	115.0581358	$\pm$ 115.0569796i	114.1630	114.5177
12	λ_1	13.1098091	$\pm$ 13.1086071i	13.5513	13.1046
	λ_2	37.0098113	$\pm$ 36.9702018i	36.8870	36.9790
	λ_3	47.8319424[a]	$\pm$ 47.8760627i[a]	—	—
	λ_4	76.3662737	$\pm$ 76.3620135i	75.3810	76.2744
	λ_5	78.5959016[b]	$\pm$ 78.5959016i[b]	—	—
	λ_6	129.9673985	$\pm$ 129.9582997i	127.3653	129.3472

[a]Torsional frequency parameter.
[b]Axial frequency parameter.

8. Results and discussion

A dynamic analysis of a rotating doubly tapered Timoshenko beam including the effects of hub radius and setting angle as well as Coriolis forces is presented. The explicit expressions for the spin and frequency parameters as well as taper ratios are given by

$$\bar{\Omega} = \Omega L^2/\sqrt{E_o/\rho A_o} \quad \text{spin parameter,}$$

$$\lambda = \omega L^2\sqrt{\rho A_o/EI_o} \quad \text{frequency parameter,}$$

$$v_y = L/L_{oy} \quad \text{taper ratio in } y\text{-direction,}$$

$$v_z = L/L_{oz} \quad \text{taper ratio in } z\text{-direction,}$$

where E is the modulus of elasticity while A_o and I_o are, respectively, the root cross-section area and the root second moment of area of the beam. The quantity ω represents the natural frequency

Table 2
The first six frequency parameters of rotating tapered Timoshenko beam $(r_g/L) = 0.02$, $\mathscr{R}_o = 0.2$, $v_y = 0.15$, $v_z = 0.30$ and $\psi = 0^\circ$

$\bar{\Omega}$	λ_i	PROM	CROM	Planar modes Full order, Eq. (41)	Complex modes Full order, Eq. (50)
3	λ_1	$\pm$ 5.049132153934i	$\pm$ 5.049132153685i	5.04914842149	$\pm$ 5.04913215368i
	λ_2	$\pm$ 21.110851583289i	$\pm$ 21.110850569280i	21.11103531306	$\pm$ 21.11085056969i
	λ_3	$\pm$ 52.869520080270i[a]	$\pm$ 52.869430842066i[a]	52.86999026431[a]	$\pm$ 52.86943083971i[a]
	λ_4	$\pm$ 58.130064927498i	$\pm$ 58.129994370448i	58.12925650161	$\pm$ 58.12999438200i
	λ_5	$\pm$ 87.021011701338i[b]	$\pm$ 87.021011701338i[b]	87.02101170134[b]	$\pm$ 87.02101170133i[b]
	λ_6	$\pm$ 98.1391903197959i	$\pm$ 98.138925800453i	98.13896566779	$\pm$ 98.13892580477i
6	λ_1	$\pm$ 7.576869248334i	$\pm$ 7.576869240697i	7.57696312507	$\pm$ 7.57686924070i
	λ_2	$\pm$ 24.536378624075i	$\pm$ 24.536374261454i	24.53729836613	$\pm$ 24.53637426119i
	λ_3	$\pm$ 56.655771464603i[a]	$\pm$ 56.655383495854i[a]	56.66165977388[a]	$\pm$ 56.65538349613i[a]
	λ_4	$\pm$ 58.136641257080i	$\pm$ 58.136360306186i	58.12925650161	$\pm$ 58.13636030465i
	λ_5	$\pm$ 87.021011701338i[b]	$\pm$ 87.021011701338i[b]	87.02101170134[b]	$\pm$ 87.02101170133i[b]
	λ_6	$\pm$ 102.249603879632i	$\pm$ 102.248487815539i	102.24877875310	$\pm$ 102.24848781632i
12	λ_1	$\pm$ 13.479261044529i	$\pm$ 13.479260800269i	13.47989501503	$\pm$ 13.47926080025i
	λ_2	$\pm$ 34.942738507006i	$\pm$ 34.942718742592i	34.94960255375	$\pm$ 34.94271874317i
	λ_3	$\pm$ 58.137062774181i[a]	$\pm$ 58.135963731111i[a]	58.12925650161[a]	$\pm$ 58.13596373427i[a]
	λ_4	$\pm$ 69.611000889220i	$\pm$ 69.608986807598i	69.61042062471	$\pm$ 69.60898680510i
	λ_5	$\pm$ 87.021011701338i[b]	$\pm$ 87.021011701338i[b]	87.02101170134[b]	$\pm$ 87.02101170133i[b]
	λ_6	$\pm$ 117.063000811815i	$\pm$ 117.057630050464i	117.06044738541	$\pm$ 117.05763005734i

[a]Torsional frequency parameter.
[b]Axial frequency parameter.

of the beam. L is the length of the beam while L_{oy} and L_{oz} are its untruncated lengths in the y- and z-directions, respectively.

The beam is of 1.0 m length and is divided into 12 equal finite Timoshenko beam elements for which Poisson's ratio $v = 0.3$, shear correction factor $\kappa = 5/6$ for rectangular cross-section and $(r_g/L) = 0.02$, in which r_g represents the radius of gyration at the root of the beam. The ratio of the modulus of elasticity to the shear modulus of rigidity (E/G) is equal to 2.6 while the mass density is taken to be 7850 kg/m^3.

The total number of degrees of freedom of such a beam is 52. When the boundary conditions are applied to a cantilever beam, the size of the system matrices given by Eq. (40) becomes of order (48×48). The planar or real eigenvalues are computed by using Eq. (41) in which the system matrices are of the same order as that of Eq. (40), resulting in 48 real eigenvalues. The complex eigenvalues are computed by means of Eq. (57) where the system matrices are of order (96×96), thus resulting in 48 conjugate pairs of pure imaginary ones which represent the natural frequencies of the beam.

A dynamic analysis program was developed to automatically generate and assemble the system matrices of Eq. (40), carry out the desired modal reduction transformations; either PROM or CROM and integrate the reduced models forward in time to predict the system's time response.

Table 3
The first six frequency parameters of rotating tapered Timoshenko beam $(r_g/L) = 0.02$, $\mathscr{R}_o = 0.2$, $v_y = 0.15$, $v_z = 0.30$ and $\psi = 90°$

$\bar{\Omega}$	λ_i	PROM	CROM	Planar modes Full order, Eq. (41)	Complex modes Full order, Eq. (50)
3	λ_1	$\pm$ 4.053373944092i	$\pm$ 4.053372643662i	4.06227844676	$\pm$ 4.05337264366i
	λ_2	$\pm$ 20.889002324294i	$\pm$ 20.888562341903i	20.89783181468	$\pm$ 20.88856234191i
	λ_3	$\pm$ 52.781755104172i[a]	$\pm$ 52.777726404445i[a]	52.78577401953[a]	$\pm$ 52.77772640435i[a]
	λ_4	$\pm$ 58.129256501613i	$\pm$ 58.129256501613i	58.12925650161	$\pm$ 58.12925650161i
	λ_5	$\pm$ 87.226990132167i[b]	$\pm$ 87.226984878754i[b]	87.02101170134[b]	$\pm$ 87.22698488229i[b]
	λ_6	$\pm$ 98.095630178560i	$\pm$ 98.089550833854i	98.09400288027	$\pm$ 98.08955083396i
6	λ_1	$\pm$ 4.589939427536i	$\pm$ 4.589934274646i	4.63057237392	$\pm$ 4.58993427463i
	λ_2	$\pm$ 23.757861694816i	$\pm$ 23.755860854642i	23.79609053463	$\pm$ 23.75586085465i
	λ_3	$\pm$ 56.329607576606i[a]	$\pm$ 56.312507036825i[a]	56.34671473899[a]	$\pm$ 56.31250703719i[a]
	λ_4	$\pm$ 58.129256501613i	$\pm$ 58.129256501613i	58.12925650161	$\pm$ 58.12925650161i
	λ_5	$\pm$ 87.845692792588i[b]	$\pm$ 87.845665549014i[b]	87.02101170134[b]	$\pm$ 87.84566555003i[b]
	λ_6	$\pm$ 102.080136305463i	$\pm$ 102.054603065903i	102.07604893610	$\pm$ 102.05460306457i
12	λ_1	$\pm$ 5.939149617108i	$\pm$ 5.939126948960i	6.15047330004	$\pm$ 5.93912694899i
	λ_2	$\pm$ 32.641045128181i	$\pm$ 32.630161418860i	32.83561434480	$\pm$ 32.63016141854i
	λ_3	$\pm$ 58.129256501613i[a]	$\pm$ 58.129256501613i[a]	58.12925650161[a]	$\pm$ 58.12925650161i[a]
	λ_4	$\pm$ 68.495204370256i	$\pm$ 68.413340343162i	68.58026115351	$\pm$ 68.41334034459i
	λ_5	$\pm$ 90.306308639939i[b]	$\pm$ 90.306191709469i[b]	87.02101170134[b]	$\pm$ 90.30619170937i[b]
	λ_6	$\pm$ 116.458667406070i	$\pm$ 116.338562887832i	116.45589814815	$\pm$ 116.33856288364i

[a]Torsional frequency parameter.
[b]Axial frequency parameter.

Table 1 shows the first four frequency parameters of a cantilever uniform Timoshenko beam rotating at different speeds using both planar and complex modes. The comparison of these frequencies shows an outstanding agreement with the numerical and exact frequencies presented by Nagaraj [34].

The first six out of plane and in-plane frequency parameters of a cantilever tapered Timoshenko beam at different spin parameters where $v_y = 0.15$, $v_z = 0.3$ and $\mathscr{R}_o = 0.2$ are shown in Tables 2 and 3, respectively. These frequency parameters, based upon reduction orders PROM = 6 and CROM = 6 compare favorably with the corresponding full order model FOM = 48. Although the reduced problem is only of order 6 (full order 48), for $\bar{\Omega} = 3$, the error in the fundamental frequency parameter in Table 2 is negligible for both PROM and CROM compared to the value obtained from the FOM of Eq. (54). The results manifest an excellent agreement between the ROM and FOM solutions. Consequently, it can be ensured from these results that the ROM preserves the characteristics of such structures.

Figs. 3–9 show the dynamic behavior of a rotating tapered cantilever Timoshenko beam for which $v_y = 0.2$, $v_z = 0.1$ and $\mathscr{R}_o = 0.1$ and rotating at a constant speed of $\Omega = 3000$ rpm for various types of input loadings applied at the midpoint of the beam.

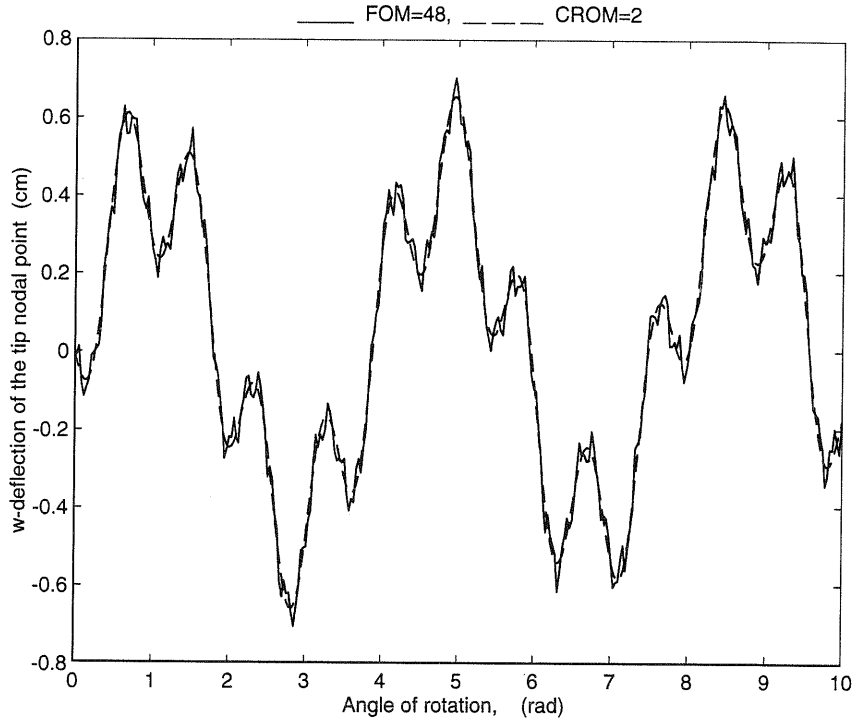

Fig. 3. Response due to impulse input.

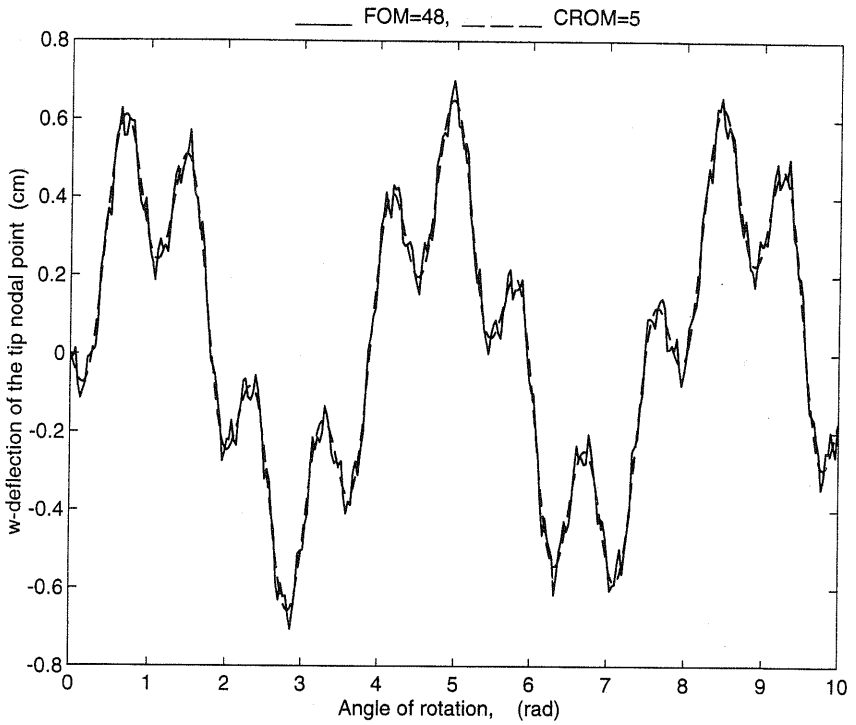

Fig. 4. Response due to impulse input.

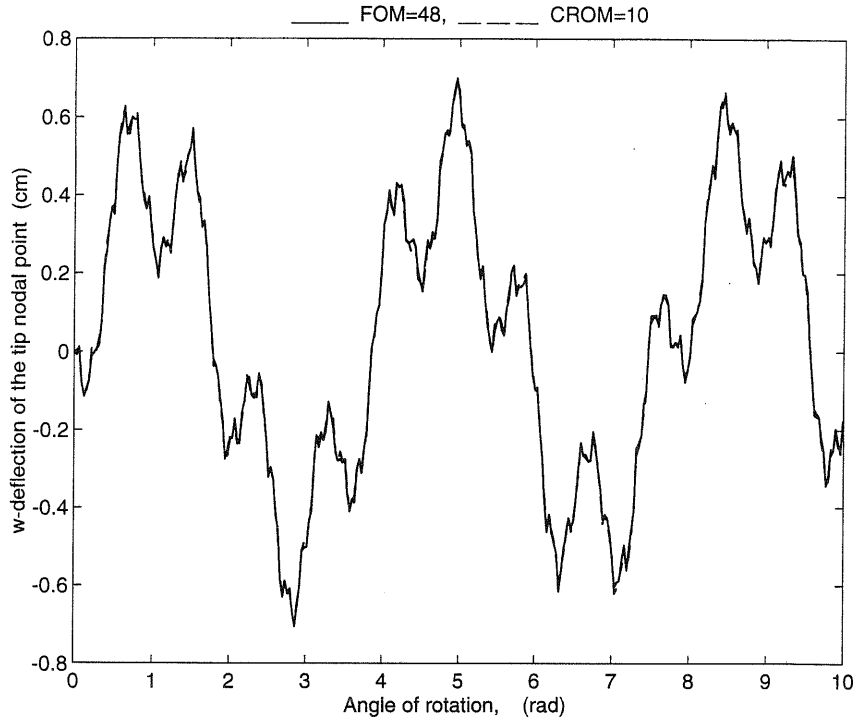

Fig. 5. Response due to impulse input.

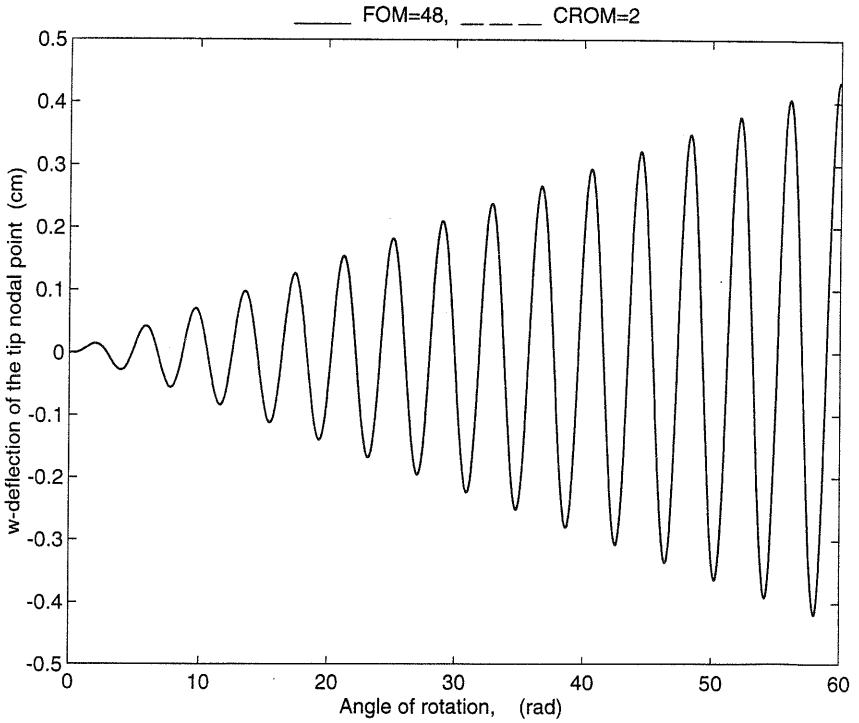

Fig. 6. Response due to sinusoidal input $F = 500 \sin(511.465t)$.

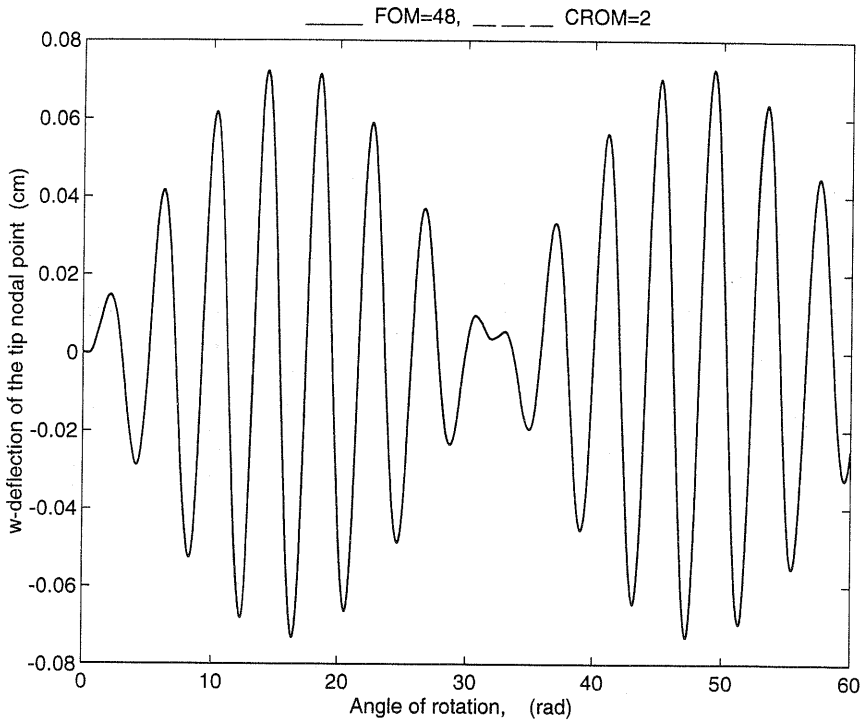

Fig. 7. Response due to sinusoidal input $F = 500\sin(450t)$.

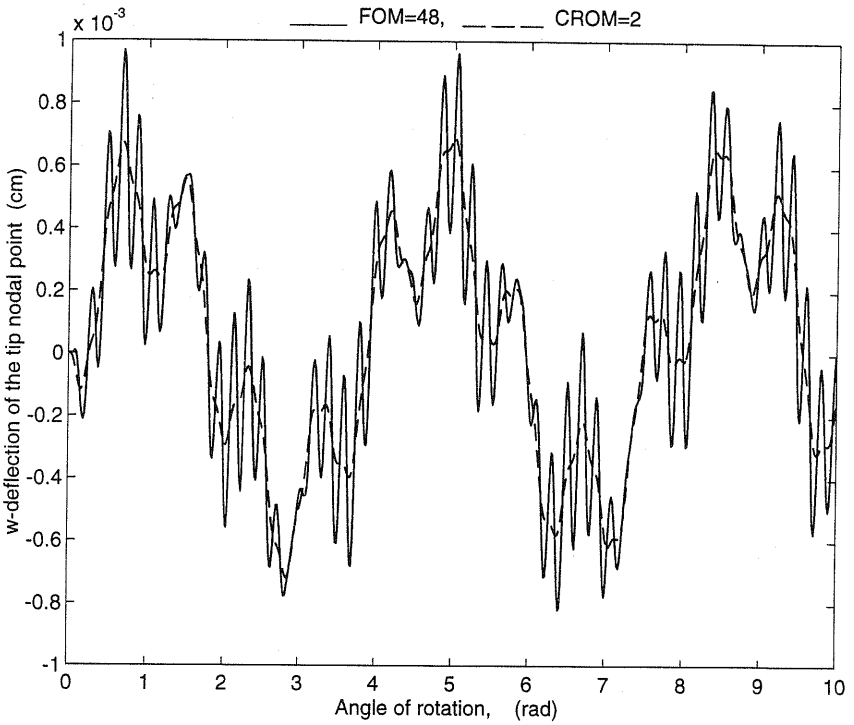

Fig. 8. Response due to sinusoidal input $F = 500\sin(9500t)$.

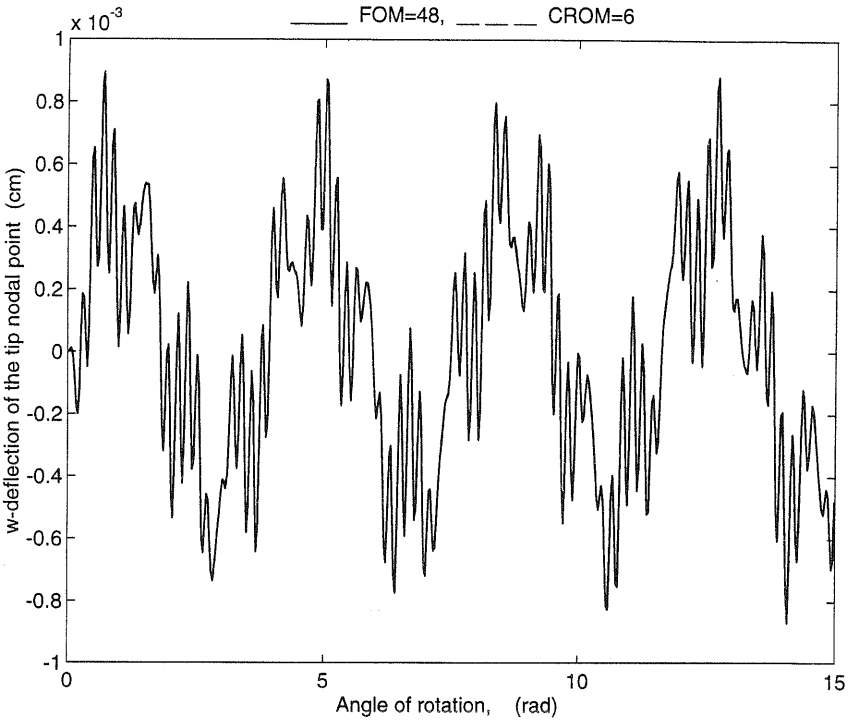

Fig. 9. Response due to sinusoidal input $F = 500 \sin(9500t)$.

Fig. 3 shows the out-of-plane flexural deformation w of the tip nodal point of the beam where the midpoint of the beam has been excited by an impulsive load of magnitude of 50 N in the vertical direction. The PROM two-mode solution matches perfectly the CROM two-mode solution, however both do not match the plot of FOM. The legend CROM on Figs. 3–9 represent the two identical responses of either CROM or PROM. It can be seen from Fig. 4 that when the retained modal coordinates have been increased to 5, the plots corresponding to the ROM still do not match exactly with the corresponding FOM plot. This is because the impulsive loading is known to excite higher modes of vibration. A further increase in the retained modes to 10 was sufficient to the response of the FOM, as shown in Fig. 5.

Fig. 6 shows the flexural deformation of the tip nodal point due to exciting the midpoint of the beam by a sinusoidal input $F(t) = 500 \sin(511.465t)N$, where $\Omega = 511.465$ rad/s is equal to the first natural frequency of the beam. As anticipated, resonance occurs as shown by both the two-mode solution and the full order solution. Fig. 7 shows a beating phenomenon when the forcing frequency of the previous applied load has been shifted to 450 rad/s. In both cases, the two-mode solutions were sufficient to obtain a perfect agreement between the ROM and the FOM.

Fig. 8 shows the flexural deformation of the tip nodal point of the beam described before under the same load conditions but for a forcing frequency of 9500 rad/s which falls between the fifth and sixth mode. In this figure, one can easily distinguish between the reduced order model and the full order model because the retained modes spectrum does not contain the forcing frequency. This renders the reduced order model "blind" to the exciting frequency and when the retained modes

have been increased to 6 it is clear that the reduced model matches perfectly with the full order model as shown in Fig. 9.

9. Conclusions

The equations of motion of a spinning tapered Timoshenko beam have been derived using the principle of virtual work. These equations include the effects of Coriolis forces, shear deformations, rotary inertia, hub radius, taper ratios and angular setting of the beam. The eigenvalue problem is solved for both full order model FOM and reduced order model ROM. Comparison is made between the two models. Based on the results of this investigation it can be concluded that the dynamic characteristics of such beams are preserved in modal reduction.

Two reduced order models using modal reduction have been successfully applied to the analysis and prediction of the vibrational response of a spinning tapered Timoshenko beam. The reduction process results in retaining a set of significant modes which account for almost the total amount of the kinetic energy content in the system. In general, the lower modes spanning the lower end of the frequency spectrum, in addition to other modes which span the frequency spectrum of the forcing function are retained as significant modes. Several types of excitation such as impulsive and sinusoidal loadings have been applied to the beam. The few retained modes are shown to preserve the exact behavior of the rotating beam for different parameter variations.

Based on the results of simulation, and within the numerical facts presented in this investigation, it can be concluded that planar modal reduction and complex modal reduction maintain the same order of comparison for this type of structures. The former is considerably easier to apply, the later is more realistic. However, for complex structures the complex modal reduction would be expected to produce more accurate results.

Acknowledgements

The authors greatly appreciate the support provided by The Mechanical Engineering Department and The Research Institute at King Fahd University of Petroleum & Minerals.

References

[1] H. Du, D. Hitchings, G.A.O. Davies, A finite element structural dynamics model of a beam with an arbitrary moving base, Part I: formulations, Finite Elements Anal. Des. 12 (1992) 118–131.

[2] H. Du, D. Hitchings, G.A.O. Davies, A finite element structural dynamics model of a beam with an arbitrary moving base, Part II: numerical examples and solutions, Finite elements Anal. Des. 12 (1992) 133–150.

[3] H.H. Yoo, R.R. Ryan, R.A. Scott, Dynamics of flexible beams undergoing overall motions, J. Sound Vib. 181 (1995) 261–278.

[4] N.L. Pedersen, M.L. Pedersen, A direct derivation of motion for 3-D flexible mechanical systems, Int. J. Numer. Methods Eng. 41 (1998) 697–719.

[5] S.H.R. Eslimy-Isfahany, J.R. Banerjee, A.J. Sobey, Response of a bending-torsion coupled beam to deterministic and random loads, J. Sound Vib. 195 (1996) 267–283.
[6] O.A. Bauchau, C.H. Hong, Nonlinear response and stability analysis of beams using finite elements in time, Am. Inst. Aeronaut. Astronaut. J. 26 (1988) 1135–1142.
[7] A.G. Hernried, W.M. Bian, A finite elements approach for determining the frequencies and dynamic response of twisted, nonuniform rotating blades with small or no precone, Comput. Struct. 48 (1993) 925–933.
[8] Z.E. Boutaghou, A.G. Erdman, A unified approach for the dynamics of beams undergoing arbitrary spatial motion, J. Vib. Acous. 113 (1991) 494–502.
[9] T.R. Kane, R.R. Ryan, A.K. Banerjee, Dynamics of a cantilever beam attached to a moving base, J. Guidance Control Dyn. 10 (1987) 139–151.
[10] L.W. Chen, H.K. Chen, Transient responses of a pre-twisted rotating blade of general orthotropy, Finite Elements Anal. Des. 13 (1993) 285–298.
[11] J. Thomas, B.A.H. Abbas, Finite element model for dynamic analysis of Timoshenko beam, J. Sound Vib. 41 (1975) 291–299.
[12] W. Carnegie, Vibrations of rotating cantilever blading: theoretical approaches to the frequency problem based on energy methods, J. Mech. Eng. Sci. 1 (1959) 225–240.
[13] A.M. Bakr, A.A. Shabana, Timoshenko beams and flexible multibody system dynamics, J. Sound Vib. 116 (1987) 89–107.
[14] W.H. Gau, A.A. Shabana, Effects of shear deformation and rotary inertia on the nonlinear dynamics of rotating curved beams, J. Vib. Acoust. 112 (1990) 183–193.
[15] Y.A. Khulief, On the finite element dynamic analysis of flexible mechanisms, Comput. Methods Appl. Mech. Eng. 97 (1992) 23–32.
[16] R.J. Guyan, Reduction of stiffness and mass matrices, Am. Inst. Aeronaut. Astronaut. J. 3 (1965) 380.
[17] B. Irons, Structural eigenvalue problems: elimination of unwanted variables, Am. Inst. Aeronaut. Astronaut. J. 3 (1965) 961.
[18] R.L. Kidder, Reduction of structural frequency equations, Am. Inst. Aeronaut. Astronaut. J. 11 (1975) 892.
[19] A.H. Flax, Comment on: reduction of structural frequency equations, Am. Inst. Aeronaut. Astronaut. J. 13 (1975) 701–702.
[20] R.L. Kidder, Reply by the author to A.H. Flax, Am. Inst. Aeronaut. Astronaut. J. 13 (1975) 701–702.
[21] A.H. Flax, Comment on: dynamic condensation, Am. Inst. Aeronaut. Astronaut. J. 23 (1985) 1841–1843.
[22] M. Paz, Reply by the author to A.H. Flax, Am. Inst. Aeronaut. Astronaut. J. 23 (1985) 1843.
[23] W.C. Hurty, Dynamic analysis of structural systems using components modes, Am. Inst. Aeronaut. Astronaut. J. 3 (1965) 678–684.
[24] R.R. Craig Jr., C.C. Bampton, Coupling of substructures for dynamic analyses, Am. Inst. Aeronaut. Astronaut. J. 6 (1968) 1313–1319.
[25] W.A. Benfield, R.F. Hruda, Vibration analysis of structures by component mode substitution, Am. Inst. Aeronaut. Astronaut. J. 8 (1971) 1255–1261.
[26] L.U. Ojalvo, M. Newman, Vibration modes of large structures by an automatic matrix-reduction method, Am. Inst. Aeronaut. Astronaut. J. 8 (1970) 1234–1239.
[27] R.M. Laurenson, Modal analysis of rotating flexible structures, Am. Inst. Aeronaut. Astronaut. J. 14 (1976) 1444–1450.
[28] P.W. Likins, Finite element appendage equations for hybrid coordinate dynamic analysis, Int. J. Solids Struct. 8 (1972) 709–731.
[29] A.A. Shabana, R.A. Wehage, A coordinate reduction technique for dynamic analysis of spatial substructures with large angular rotations, J. Struct. Mech. 11 (1983) 401–431.
[30] K. Kane, B.J. Torby, The extended modal reduction method applied to rotor dynamic problems, J. Vib. Acoust. 113 (1991) 79–84.
[31] Y.A. Khulief, M.A. Mohiuddin, On the dynamic analysis of rotors using modal reduction, Finite Element Anal. Des. 117 (1997) 41–55.
[32] A. Bazoune, Y.A. Khulief, A finite beam element for vibration analysis of rotating tapered timoshenko beams, J. Sound Vib. 156 (1992) 141–164.

[33] A. Bazoune, Y.A. Khulief, N.G. Stephen, Further results on modal characteristics of rotating tapered Timoshenko beams, J. Sound Vib. 219 (1999) 155–172.
[34] V.T. Nagaraj, Approximate formula for the frequencies of a rotating Timoshenko beam, J. Aircraft 33 (1996) 637–639.
[35] M.A. Mohiuddin, Finite element analysis of multibody rotor-bearing system with cracked shaft, Ph.D. Dissertation, KFUPM, 1997.